Immune checkpoint CD155 promoter methylation profiling reveals cancer-associated behaviors within breast neoplasia

Reference:
Triki Hana, Declerck Ken, Charfi Slim, Ben Kridis Wala, Chaabane Kais, Ben Halima Sawssan, Sellami Tahya, Rebai Ahmed, Vanden Berghe Wim, Cherif Boutheina.- Immune checkpoint CD155 promoter methylation profiling reveals cancer-associated behaviors within breast neoplasia
Cancer immunology and immunotherapy - ISSN 1432-0851 - New york, Springer, 71:5(2022), p. 1139-1155
Full text (Publisher's DOI): https://doi.org/10.1007/S00262-021-03064-6
To cite this reference: https://hdl.handle.net/10067/1825480151162165141

Title: Immune checkpoint CD155 promoter methylation profiling reveals cancer-associated behaviors within breast neoplasia

Running title: CD155 promoter methylation in breast cancer

Authors:

Hana Triki [1], Ken Declerck [2], Slim Charfi [3], Wala Ben Kridis [4], Kais Chaabane [5], Sawssan Ben Halima [5], Tahya Sellami [3], Ahmed Rebai [1], Wim Vanden Berghe [2], Boutheina Cherif [1,] *

Authors' affiliation:

[1]Laboratory of Molecular and Cellular Screening Processes, Centre de Biotechnologie de Sfax, University of Sfax, Sfax, Tunisia.

[2]Laboratory of Protein Chemistry, Proteomics and Epigenetic Signaling (PPES) and Integrated Personalized and Precision Oncology Network (IPPON), Department of Biomedical Sciences, University of Antwerp, Antwerp, Belgium.

[3]Department of Pathology, University Hospital Habib Bourguiba, Sfax, Tunisia.

[4] Department of Medical Oncology, University Hospital Habib Bourguiba, Sfax, Tunisia

[5] Department of Gynecology, University Hospital Hédi Chaker, Sfax, Tunisia

***Corresponding author:**

E-mail: boutheina.cherif@isbs.usf.tn
boutheina.cherif.cbs@gmail.com

Phone: (+ 216) 99 825 555
Fax: (+ 216) 74 87 58 18
Postal Address: Center of Biotechnology of Sfax, B.P 1177 Sfax 3018 Tunisia

ABSTRACT

BACKGROUND: CD155 immune checkpoint has recently emerged as a compelling immunotherapeutic target. Epigenetic DNA methylation changes are recognized as key molecular mechanisms in cancer development. Hence, the identification of methylation markers that are sensitive and specific for breast cancer may improve early detection and predict prognosis. We speculate that CD155 promoter methylation can be a valuable epigenetic biomarker, based upon strong indications for its immunoregulatory functions.

METHODS: Methylation analyses were conducted on 14 CpGs sites in the CD155 promoter region by bisulfite pyrosequencing. To elucidate the related gene expression changes, a transcriptional study using RT-qPCR was performed. Statistical analyses were performed to evaluate correlations of CD155 methylation profiles with mRNA expression together with clinical-pathological features, prognosis and immune infiltrate.

RESULTS: CD155 promoter methylation profile was significantly associated with SBR grade, tumor size, molecular subgroups, HER2 and hormonal receptors expression status. Low CD155 methylation rates correlated with better prognosis in univariate cox proportional hazard analysis, and appeared as an independent survival predictor in cox-regression multivariate analysis. Further, methylation changes at CD155 specific CpG sites were consistent with CD155 membranous mRNA isoform expression status. Statistical analyses also showed a significant association with immune Natural Killer cell infiltrate when looking at the CpG7, CpG8, CpG9 and CpG11 sites.

CONCLUSION: Altogether, our results contribute to a better understanding of the impact of CD155 immune checkpoint modality expression in breast tumors, revealing for the first time that specific CpG sites from CD155 promoter may be a potential biomarker in breast cancer monitoring.

Key words: CD155; immune checkpoint; DNA methylation; mRNA expression; breast cancer

Abbreviations: Tumor Infiltrating Lymphocytes, TILs; NK, Natural Killer; NK-TILs, Tumor-Infiltrating Natural Killer Cell; Tumor Microenvironment, TME; membranous CD155, *m*-CD155; cytoplasmic CD155, *cyt*-CD155; Overall Survival, OS; Disease-Free Survival, DFS; Scarff-Bloom-Richardson, SBR; tumor, lymph node and metastases, TNM; Luminal A, LA; Luminal B like, LB-Like; HER2 positive, HER2; Triple Negative breast cancer, TNBC; Formalin-Fixed and Paraffin-Embedded, FFPE; Beta-Actin, ACTB; real-time Quantitative Reverse Transcriptase Polymerase Chain Reaction, RT-qPCR; base pair, bp; Kilobase pair, kbp, TBE, Tris-Borate-EDTA.

Declarations

Funding sources

This work was financially supported by ISESCO (Islamic Educational, Scientific and Cultural Organization) Research grant (Ref N°2148).

Conflicts of interest disclosure

The authors have no conflicts of interest to declare.

Availability of data and material

All data generated or analyzed during this study are included in this published article.

Authors' contributions

Hana Triki: Data curation, Formal Analysis, Investigation, Methodology, Software, Validation, Visualization, Writing – original draft, Writing – review and editing. **Ken Declerck:** Formal Analysis, Software, Visualization. **Slim Charfi:** Data Curation, Project administration, Resources, Supervision, Validation. **Kais Chaabane:** Data curation, Resources. **Sawssan Ben Halima:** Data curation, Resources. **Wala Ben Kridis:** Data curation, Resources. **Tahya Sellami:** Data curation, Resources. **Ahmed Rebai:** Formal Analysis, Project administration, Supervision, Validation. **Wim Vanden Berghe:** Project administration, Resources, Supervision, Validation, Visualization, Writing – review and editing. **Boutheina Cherif:** Conceptualization, Funding acquisition, Investigation, Methodology, Project administration, Resources, Supervision, Validation, Visualization, Writing – review and editing.

Ethics approval

All procedures performed in studies involving human participants were in accordance with the ethical standards of the institutional and the national research committee of Habib Bourguiba University Hospital and with the 1964 Helsinki declaration and its later amendments or comparable ethical standards. Sampling was made only on patient tissues from tissue library of Pathology Department-Habib Bourguiba Hospital and no samples were made specifically for the study.

Consent to participate

We have conducted a retrospective study, for this type of study formal consent is not required.

Consent for publication

All authors reviewed and approved the manuscript for submission.

105 **INTRODUCTION**

106 Immune checkpoint molecules act in co-stimulatory and inhibitory pathways that tightly regulate the
107 immune response and maintain self-tolerance under normal physiological conditions. Tumors have been
108 shown to dysregulate these pathways to build immune resistance mechanism creating an
109 immunosuppressive microenvironment leading to immune evasion of cancerous cell [1], [2]. Indeed,
110 extensive studies revealed a crucial role for the immune system both in tumor suppression and promotion,
111 by regulating adaptive and innate immune pathways involving especially T cells and Natural killer (NK)
112 cells. Therefore, immune checkpoints molecules which target these immunoregulatory pathways hold
113 promise to strengthen the body's immunological function against tumors [3].

114 The most known immune checkpoint regulators are programmed cell death 1 (PD-1)/PD-1 ligand 1 (PD-
115 L1), cytotoxic T lymphocyte antigen-4 (CTLA-4), T cell immune-receptor with immunoglobulin (Ig) and ITIM
116 domains (TIGIT) [4], [5] and several others are currently being evaluated as potential therapeutic targets
117 to improve the anti-tumor immunity. Recently, TIGIT and its ligand poliovirus receptor (PVR, CD155) have
118 entered the limelight as novel immune checkpoints [6]. Besides, CD155 has an immunoregulatory potential
119 upon interaction with the co-stimulatory immune receptor CD226 (DNAM-1) and the inhibitory checkpoint
120 receptors TIGIT and CD96, which are differentially regulated at the cell surface of NK cells and T cells [6],
121 [7]. The integration of signals from CD155 cognate receptors results in activation or inhibition of NK cell
122 mediated innate immunity. In addition, CD155 overexpression has also been observed in various tumor
123 types, including colon cancer, lung adenocarcinoma, melanoma, pancreatic cancer glioblastoma [8]–[12]
124 and breast cancer [13]–[15]. Interestingly, we have recently reported the clinical significance and the
125 prognostic value of CD155 protein expression in human breast cancer [14]. CD155 can be expressed in the
126 cytoplasm or at the plasma membrane level, suggesting different immunoregulatory roles in the tumor
127 microenvironment. Moreover, CD155 undergoes alternative splicing, generating four unique splice
128 isoforms [16], [17]. It can be produced as soluble forms lacking the transmembrane domain, encoded by
129 alternative splicing isoforms β and γ [18], or as a membrane-bound protein encoded by two alternative
130 splicing forms, α and δ, referenced as the transmembrane isoforms [17]. Whereas transmembrane CD155
131 acts as an activating ligand of NK cells and cytotoxic T lymphocytes (CTLs), other studies suggest that
132 overexpression of soluble CD155 isoforms could act as a cancer-specific immune resistance mechanism
133 against the cell mediated immune response by masking the signaling effect of transmembrane CD155
134 isoform [19].

135 Moreover, expression of immune checkpoint molecules is further controlled by epigenetic mechanisms
136 which add another regulatory layer to immune modulation. Since aberrant

137 hypermethylation/hypomethylation patterns frequently result in adverse tumorigenic gene expression
138 and impaired immune checkpoint regulation, differentially methylated loci might represent useful
139 biomarkers in immune-oncology [20], [21]. More precisely, studies showed that altered gene expression,
140 and/or deregulated epigenetic machineries display central roles in the onset and progression of breast
141 cancer [22]. Particularly, DNA promoter methylation studies in patients with breast cancer using normal
142 and cancer tissues showed hypomethylation irrespective of the immune checkpoint PD-L1 expression
143 status [23]. Accordingly, a number of clinical biomarker assays are needed for early detection and to
144 predict prognosis of cancer, combining therapies of DNA demethylating agents with immune checkpoint
145 inhibitors [24], [25].
146 Therefore, we studied the differential expression of immune checkpoint CD155 in relation to its promoter
147 methylation pattern in breast cancer patients.

148 **MATERIAL AND METHODS**

149 **Study population and tumor samples**

150 This is a retrospective cohort study of females diagnosed with invasive breast carcinoma who underwent
151 surgical resection prior to any treatment at the Department of Gynecology and Obstetrics of the Hedi
152 Chaker University Hospital in the south of Tunisia. All procedures performed in this study were in
153 compliance with the ethical standards of the institutional and the national research committee of Habib
154 Bourguiba University Hospital and with the 1964 Helsinki declaration and its later amendments or
155 comparable ethical standards. We collected a total of n = 116 well characterized primary breast cancer
156 tissues, and n =11 non-tumor breast tissue samples from women without cancer used as healthy control.
157 Samples were retrieved from the tumor bank of the Department of Pathology of the Habib Bourguiba
158 University Hospital (Sfax, Tunisia) and they included 101 frozen tissues and 15 formalin-fixed and paraffin-
159 embedded (FFPE) tissues. The clinical pathological data acquired by retrospective medical records included
160 age, histological grade, histological type, molecular subtype, tumor size, lymph node status, distant
161 metastasis, lymphovascular invasion, menopausal status, adjuvant therapy status and clinical stage
162 according to the 8th edition of TNM (tumor, node, metastasis) classification adopted by the International
163 Union Against Cancer. The clinical-pathological characteristics of 116 breast cancer patients are
164 summarized in Supplementary Table 1. Overall survival (OS) and disease-free survival (DFS) were
165 investigated to evaluate CD155 influence upon patient prognosis at the department of medical oncology
166 of the Habib Bourguiba University Hospital (Sfax, Tunisia). The overall follow-up time ranged from 1 to 151

167 months, with a median follow-up of 78.5 months, during which 25 patients underwent cancer relapse and
168 29 died.

169 **Breast cancer subtyping**

170 Breast cancer molecular classification is based on the expression of classical biomarkers including estrogen
171 (ER) and progesterone (PR) receptor, the human epidermal growth factor receptor 2 (HER2) and Ki-67
172 labeling index as a cell proliferation biomarker. Expression of all biomarkers was carried out using
173 immunohistochemical method. Hormone receptors (ER and PR) were considered positive when >1% of
174 infiltrating tumor cell nuclei were stained. Tumors were considered positive for HER2 if immunostaining
175 was scored as 3+ according to Wolff criteria [26] and cancers with HER2 scored as 2+ (indeterminate) were
176 assessed through fluorescent in situ hybridization [FISH]. Ki-67 was visually scored for percentage of tumor
177 cell nuclei with positive immunostaining above the background level using a cutoff at 20% of expression.
178 Five molecular subtypes were defined: Luminal A (LA) if ER/PR+, HER2- and Ki-67 < 20%; Luminal B like (LB-
179 Like) if ER/PR+, HER2− and Ki-67 > 20%; Luminal B (LB) if ER/PR+ and HER2+; HER2 positive (HER2) if ER/PR
180 − and HER2+; Triple Negative Breast Cancer (TNBC) if ER/PR− and HER2− as described previously [14].
181

182 **Immune infiltrate evaluation**

183 TILs evaluation was performed by a standardized methodology which relies on visual assessment of
184 hematoxylin and eosin sections. According to the international TILs Working group recommendations (ref),
185 TILs were detected by a semiquantitative evaluation by light microscopy. Briefly, all inflammatory
186 mononuclear cells in the stromal compartment within the borders of the invasive tumor were evaluated
187 and reported as a percentage than as a level (TILs grade). TILs outside the tumor border, around ductal
188 carcinoma in situ and normal breast tissue, as well as in areas of necrosis were not taken into account. TILs
189 expression levels were classified into 3 grades: low (0-10%), medium (10%-50%), and high (50%-90%) as
190 described previously [27]. NK-TILs infiltration was assessed by immunohistochemistry using the anti-CD56
191 antibody (NCL-L CD56-1B6, Leica Novocastra). NK-TILs were evaluated as CD56+ lymphocytes tissues count
192 and distribution in ten randomly selected areas, and then evaluated at higher magnification (×40
193 objectives). Scoring of NK-TILs immunostaining was determined as low (negative or weak) cell presence or
194 high (moderate or strong) cell presence by a cut-off value of five cells as described previously [14].

195

196

197 **DNA extraction and qualification**

198 Five 10 µm thick OCT (Optimal Cutting Temperature compound) embedded frozen tissue and FFPE tissue
199 sections were cut for each case. Sample matched genomic DNA was extracted by standard Proteinase K
200 digestion with slight modification [28], followed by phenol–chloroform extraction and ethanol
201 precipitation. FFPE tissues were deparaffinized in xylene followed by subsequent rehydration through
202 graded alcohols prior to any extraction step. For each case, tissues were homogenized in 490 µl of
203 proteinase K buffer (0.5M EDTA pH 8, 2M Tris, 1.5M NaCl, H2O) with a mixer mill (MM 400, RETSCH) using
204 adapter Rack for 10 Reaction Vials and 10 mm stainless steel grinding balls at 30 Hz for 1 min. Samples
205 were then incubated with 10 µl proteinase K (20mg/ml) at 56°C for four hours, after incubation the tissue
206 dissolves completely. DNA was extracted by adding an equal volume of phenol-chloroform-isoamyl alcohol
207 (25: 24: 1) and precipitated overnight with sodium acetate and ethanol at −20°C. The DNA pellet of each
208 sample was collected by centrifugation for 20 minutes at 4°C, purified with cold 70% ethanol and air dried
209 at room temperature. DNA was resuspended in 20 µl of sterile distilled water. Extraction yield was
210 evaluated with Nanodrop 2000 spectrophotometer (Thermo Scientific, Wilmington, DE, USA). Extracted
211 DNAs were then assessed for their integrity by a control PCR reaction designed to amplify a fragment of
212 250 bp of the β-globin gene as described previously [29].

213 **DNA bisulfite conversion and qualification**

214 Genomic DNA (500 ng) was bisulfite converted using the EZ DNA methylation kit (Zymo Research,
215 Cambridge Bioscience, Cambridge, UK) according to manufacturer's instructions. Bisulfite-treated
216 genomic DNA was re-quantified using a Qubit 4.0 fluorometer (Life Technologies) according to the
217 manufacturer's protocol. Successful bisulfite conversion was confirmed by the amplification of a 208 bp
218 amplicon of the *SALL3* gene as described previously [30], under the following conditions: 95°C 15 min; then
219 45 cycles of 94°C 30 sec, 55°C for 30 sec, 72°C for 30 sec; followed by 72°C for 10 min using the primer
220 set: *SALL3*-Fw:5'-GTTTGGGTTTGGTTTTTGTT-3'; *SALL3*-Rev:5'-ACCCTTTACCAATCTCTTAACTTTC-3'.
221 Successful PCR amplification was evaluated by TBE (Tris-Borate-EDTA) electrophoresis at 2% agarose gel
222 and visualized by GelRed™ staining.

223 **CD155 pyrosequencing**

224 For CpG site-targeted bisulfite pyrosequencing, we used the PyroMark assay design 2.0 software for
225 forward, biotinylated-reverse and sequencing CD155 primers design. Targets of interest were PCR

226 amplified using the PyroMark PCR kit (Qiagen, Hilden, Germany) according to manufacturer's instructions.
227 For each sample, 50 ng of bisulfite-treated DNA was subsequently used for PCR amplification in a final
228 volume of 25 µL containing 10 µM of forward primer and biotin-labeled reverse primer. The primers
229 sequences are summarized in Table 1. Cycling conditions started with an initial PCR activation at 95°C for
230 15 min, then 45 cycles of 95°C for 30 sec, 56°C for 30 sec, 72°C for 30 sec, followed by a final extension at
231 72°C for 10 min. Successful PCR amplification was confirmed by TBE electrophoresis at 2% agarose gel and
232 visualized by GelRed™ staining.
233 After the amplification, pyrosequencing was performed using the PyroMark Advanced Q24 System
234 according to the manufacturer's guidelines (Qiagen, Hilden, Germany). In brief, Biotin-labeled PCR
235 products were immobilized on Streptavidin-coated Sepharose beads (High Performance, GE Healthcare,
236 Uppsala, Sweden) in the PyroMark binding buffer (Qiagen, Hilden, Germany). The mixtures were agitated
237 at room temperature for 15 min under constant mixing (1400 rpm). The DNA-coated beads were
238 subsequently captured by the PyroMark vaccum Q24 workstation, washed and denaturated. The beads
239 with single-stranded DNA templates were then released into a 24-well plate with 20 µl of PyroMark
240 annealing buffer (Qiagen, Hilden, Germany) containing the corresponding sequencing primer at a final
241 concentration of 0.4 µM (Table 1) for 2 min at 80°C. The PyroMark plate was placed into a PyroMark Q24
242 Advanced instrument (Qiagen, Hilden, Germany) and the sequencing procedure was performed by the
243 cyclic dispensation of substrates, enzymes, and four different nucleotides in a pre-specified order
244 (PyroMark Advanced Reagents, Qiagen, Hilden, Germany). Following pyrosequencing, the completed run
245 files were imported into PyroMark Q24 Advanced software (version 3.0.0; Qiagen) and cytosine
246 methylation was quantified.

247 **RNA extraction and real-time reverse transcriptase polymerase chain reaction analysis**

248 Frozen tissues (30 mg) were disrupted using a mixer mill (MM 400, RETSCH) until they are uniformly
249 homogeneous. Total RNA was isolated from frozen tissues using the AllPrep DNA/RNA Mini Kit (Qiagen)
250 according to the manufacturer's protocol. Extraction yield was evaluated with Nanodrop 2000
251 spectrophotometer (Thermo Scientific, Wilmington, DE, USA). First-strand cDNA was synthesized from 1µg
252 of total RNA using PrimeScript RT reagent Kit (Takara Bio Inc., Otsu, Japan) according to the manufacturer's
253 recommendations. cDNAs were used as template for PCR using specific primers for CD155 and β-Actin
254 (housekeeping gene/endogenous control). All samples were done in duplicate for both target and
255 reference gene. Real-time quantitative PCR (RT-qPCR) were performed in a CFX96 Real Time PCR detection
256 system (Bio-Rad, Hercules, CA, USA) and carried out in a final volume of 10 µl using 5ng of cDNA, 0.3µl of

257 each primer (10 µM), 5 µl of the TB Green Premix Ex Taq II (TliRNaseH Plus, Takara Bio, Japan) and RNase
258 free water (DEPC-Treated). The thermal cycling conditions were as follows: 30 s at 95°C and 39 cycles of
259 10 s at 95°C, 30 s at 64°C and 5 s at 72°C.
260 CD155 primer set was carefully designed to amplify relevant transcripts without genomic DNA
261 contamination. PCR primer sequences were as follows: *CD155*-Fw: 5'- ACTCAGGCATGTCCCGTAAC-3'
262 and *CD155*-Rev: 5'- CTGTACTCGAGGGACACAGATG-3'; for β-Actin amplification the following primer
263 set was used: *β-Actin*-Fw: 5' -CATCGAGCACGGCATCGTCA -3' and *β-Actin*-Rev: 5' -
264 TAGCACAGCCTGGATAGCAAC-3' (211bp). Melt curve analysis was performed for all PCR products following
265 RT-PCR run using the Bio-Rad CFX Manager software 3.1 (Bio Rad, Redmond, WA, USA). The CD155 mRNA
266 expression level is given as relative copy numbers normalized against β-Actin housekeeping gene
267 transcripts.

268 **Statistical analysis**

269 The methylation data imported into R studio (version 3.6.1) were processed, correlations of the
270 methylation percentages results with patients clinical-pathological features and with CD155 expression
271 levels were assessed with Student's t test and Anova test.
272 In multivariate analysis, the calculation of the hazard ratios and their 95% confidence interval was carried
273 out using a Cox model. Survival analyses were performed using SPSS 20.0 statistical software for Windows
274 (SPSS Inc., IBM).
275 For all the statistical tests used in this work, associations were retained as significant for a p-value ≤ 0.05.

276 **RESULTS**

277 **Genomic designing and technical concept for CD155 promoter methylation analysis**

278 Primer sets with one biotin-labelled primer were used to amplify the bisulfite converted DNA. New primers
279 for CD155 gene were designed using PyroMark Assay Design software version 2.0 (Qiagen), amplicons
280 were kept short with lengths between 90 and 150 base pairs (bp) to enable subsequent studies on FFPE
281 specimens. Primers were located in promoter CpG islands identified by MethPrimer, depending on where
282 the design of the assay allowed for optimal primers. Due care was taken to avoid any primer overlapping
283 CG dyads to prevent amplification biases.
284 The choice of the genomic region sensitive to methylation was carried out by the CpGs island prediction
285 software the Li Lab Tools and Databases (http://www.urogene.org/cgi bin/methprimer/methprimer.cgi).

286 CD155 genomic sequence was extracted from genomic databases (Genome Browser) by adopting the
287 annotation proposed by Ensembl genome browser (http://www.ensembl.org). Selection was performed
288 on the entire genomic sequence with the addition of 2 kbp in upstream of its first ATG.
289 Li Lab Tools Software displays the potential CpGs islets of the submitted selection, regions with the highest
290 score were considered for primers design. The in-silico study showed that the CD155 gene has 8 exons and
291 7 introns and that the first 2000 nucleotides of its promoter contain a single CpG island (Figure 1).
292 Regions of interest were then submitted to the software provided by Qiagen "PyroMark Assay Design 2.0".
293 The corresponding converted sequence after bisulfite treatment were provided and the corresponding
294 primer sets are automatically generated containing both PCR primers and sequencing primers. Each set of
295 primers is associated with a quality index assigned in the form of a score based on several parameters
296 specific to the pyrosequencing analysis. The selected primer set had a score equal to 80%. The reverse
297 primer of the selected primer set has the particularity of being coupled to a biotin molecule, allowing its
298 purification during pyrosequencing. We quantified methylation percentages of the CpG sites of CD155
299 gene promoter by pyrosequencing using a CD155 sequencing primer. The targeted region in our study
300 displays 14 CpG sites (Figure 1). According to UCSC genome browser and ENCODE data, this region is
301 located in a CpG island encompassing several enhancers and regulatory elements, suggesting that this
302 region is involved in the active transcription of CD155.

303 **Evaluation of CpG sites methylation rates of CD155 gene promoter by pyrosequencing**

304 CD155 promoter methylation was investigated in 116 primary breast carcinoma samples taken from FFPE
305 and frozen cancerous breast tissue biopsies. In addition, 11 healthy breast samples taken from frozen
306 tissues were included in our study as healthy controls. The pyrograms obtained display methylation rates
307 calculated by comparing the heights of C and T peaks at each CpG site. The results of pyrosequencing of
308 the selected region show that the methylation rates are relatively low and range between 1 to 46%. FFPE
309 samples were successfully analyzed and were therefore included for pyrosequencing analysis, samples
310 ranged in their degree of methylation between 0% and 43.02%. Likewise, frozen samples were successfully
311 analyzed and were further investigated for their promoter methylation. Frozen cancerous breast tissue
312 DNAs ranged in their degree of methylation between 0% and 45.83%, while healthy frozen samples ranged
313 between 0% and 30.08%. To ensure our results credibility, samples were pooled for subsequent analyses
314 taking into account the significant difference between FFPE and frozen samples using correction
315 coefficient.

316 Statistical analyses showed no evidence for significant differences in global methylation level (overall
317 methylation mean percentage) of cancer tissues as compared to healthy controls, although cancer tissues
318 were slightly higher in methylation (*p*-value = 0.508)

319 **Association between CD155 methylation status, clinical indicators and immune infiltrate data**

320 Table 2 summarizes all the correlations established between the CD155 gene promoter CpG sites
321 methylation status, and the clinico-pathological data. We evaluated the differences in global DNA
322 methylation according to clinical-pathological features. Although methylation appeared to be higher for
323 the tumor SBR grades II and III, the correlation did not reach statistical significance (*p*-value = 0.064, Fig 2,
324 a). However, a significant correlation was found between CD155 methylation status and tumor size where
325 higher levels of methylation were correlated with higher tumor size (*p*-value = 0.001, Fig 2, b).
326 Statistical analyses also showed a significant association with molecular groups. Most importantly, the
327 Her2, LB and TNBC groups had almost the same trend with higher global methylation rates compared to
328 the LB-like and LA groups (*p*-value = 0.00343, Fig 2, c). On the other hand, statistical analysis showed a
329 significant and positive correlation between a higher methylation and the expression of the HER2 receptor
330 (*p*-value = 0.005, Fig 2, d). Meanwhile, negative correlations with progesterone (RP) and estrogen (RE)
331 receptors expression status (*p*-value = 0.007 and *p*-value = 0.03, respectively, Fig 2, e-f) were found.
332 Next, we assessed the difference in overall methylation mean percentage according to Tumor infiltrating
333 lymphocytes (TILs) and NK cells (NK-TILs) in breast cancer patients. No association with the immune
334 infiltrate was found (Table 2).

335 **Profiling of differentially methylated CpG sites related to clinical-pathological data**

336 We determined which of the 14 individual CpG sites were better suited to be related to clinical-
337 pathological indicators, we therefore scanned the entire region to refine our search. Table 3 reports the
338 different correlations between the methylation rates of the 14 individual CpG sites and clinical-
339 pathological features. With SBR grade, a statistically significant difference in methylation between the
340 three groups was observed when looking at CpG7 and CpG9 (*p*-value = 2.17e-2, *p*-value = 2.46e-2,
341 respectively) with the same trend observed when comparing global methylation mean percentage with
342 SBR grade. Moreover, a significant correlation was found with molecular group, this difference is observed
343 in almost all CpG sites particularly in CpG1, CpG3 to CpG10, CpG12 and CpG13. Statistical analysis also
344 demonstrated significant associations with the expression of the HER2 receptor, a positive correlation
345 between higher methylation rates and a HER2 + status was observed, the differences were significant for

346 CpG2 to CpG10 and CpG13 sites. On the other hand, a negative correlation with the receptors of RP and
347 RE was found where RE + and RP + tumors were lower in methylation at CpG1, CpG3 to CpG9 and CpG13
348 sites for the RE receptor, and the CpG4 to CpG9 and CpG13 sites for the RP receptor. In addition, a
349 significant association was found between methylation status of all CpG sites and tumor size where larger
350 tumors were higher in methylation compared to tumors with lower size. Further, we found a significant
351 association with metastasis when looking at CpG4 where a higher methylation percentage correlated
352 positively with metastasis.
353 Statistical analyses also showed a significant association with NK cell infiltration when looking at the CpG7,
354 CpG8, CpG9 and CpG11 sites (*p*-value = 3.53e-2, *p*-value = 0.0347, *p*-value = 1.39e-2 and *p*-value = 0.0119,
355 respectively), where we noted a correlation between a higher methylated status and a dense infiltrate of
356 NK-TILs (Figure 3, a-d).

357 These results showed that the methylation percentages of CpG4 to CpG9 sites were better suited to be
358 associated with clinical-pathological parameters than the average global CD155 methylation percentage.
359 Therefore, CpG4 to CpG9 sites mean percentage methylation was used in the subsequent analyses. Thus,
360 all analyses were performed with the average (sub_mean) of CD155 methylation over all six CpGs (CpG4
361 to CpG9) and this did not affect the general conclusions (Table 2).

362 **CD155 membranous mRNA isoform expression analysis**

363 We studied the expression profile of CD155 by quantitative real-time PCR. We already highlighted that
364 CD155 is expressed in several isoforms corresponding to splicing variants, it is expressed at the cytoplasmic
365 or membrane level, this localization is tightly related to these isoforms. In fact, CD155 undergoes
366 alternative splicing, generating four unique splicing isoforms. It can be expressed in a soluble form lacking
367 a transmembrane domain, encoded by alternative splice isoforms β and γ, or as a membrane bound
368 protein encoded by two alternative splicing isoforms, α and δ. To analyze the relative expression of CD155
369 transcripts, we designed a primer set which amplifies cDNA but not genomic DNA. This primer set amplifies
370 the sequence that covers the transmembrane domain, one primer of this set is located on exon 6 which
371 corresponds to the transmembrane domain (α isoform) while the other is located on the junction exon 6
372 – exon 7. CD155 transcripts were detected in most patients, although at different levels. The relative
373 expression of each gene was normalized with respect to the housekeeping gene β-Actin (ACTB). The overall
374 transcriptome patterns displayed a similar distribution of the normalized intensity values among all
375 samples with no significant differences between the affected and control groups (*p*-value= 0.50). Relative
376 mRNA abundance was determined by the $2^{\Delta\Delta Cq}$ method ($\Delta\Delta Cq_x$: [Cq_x gene test−Cq_x endogenous control] −

377 mean of ΔCq healthy control), and results are summarized as the mean ± s.d of two independent
378 experiments. Correlations of CD155 mRNA expression profile with clinical indicators are summarized in
379 Table 2. The only significant association was observed with histological type (*p*-value= 0.045).

380 **Correlations between DNA hypomethylation variations and transcriptional expression data**

381 CD155 mRNA transcripts were analyzed to verify possible associations with global changes in DNA
382 methylation levels (sub_mean methylation percentage) for each patient. Samples lacking DNA methylation
383 revealed relatively higher trend of CD155 transcription levels though not statistically significant (*p*-value:
384 0.370, Figure 4, a). Consistent with these results, patients with strongest transcription levels for this
385 checkpoint molecule were highly hypo-methylated, when methylation was dichotomized according to its
386 median into highly or weakly hypomethylated tumors (*p*-value =0.159, Figure 4, b).
387 Altogether, association between methylation and transcription levels for this gene was found insignificant,
388 suggesting that CD155 expression might not be exclusively regulated by DNA methylation.

389 **Correlations between CD155 membranous mRNA isoform expression and protein localization**

390 We have earlier reported CD155 protein expression as strong prognostic parameter that is associated with
391 breast cancer progression and patient's outcome. Beforehand, we characterized two protein localizations
392 via an immunohistochemistry detection method (IHC), which showed different contributions of each
393 isoform in BC progression [14]. This prompted us to investigate potential correlations between CD155
394 membranous mRNA isoform expression and protein localization. Therefore, we attempted to confirm
395 whether CD155 membranous mRNA isoform expression is related to protein localization. To this end, we
396 assessed the correlations between CD155 mRNA expression levels and CD155 protein expression. Despite
397 the limited statistical significance, our results suggest that CD155 membranous mRNA isoform expression
398 is positively related to membranous CD155 (m-CD155) protein localization, where high m-CD155 protein
399 expression tumors reveal high transcription levels which are clearly reduced in tumors with high
400 cytoplasmic CD155 protein expression (cyt-CD155). Although there was no significant correlation with
401 transcription levels for both protein localizations, Fig. 5a, b shows a clear reciprocal trend, although with
402 poor statistical significance.

403 **CD155 promoter methylation impact on patient's outcome**

404 Overall survival (OS) and disease-free survival (DFS) were investigated by survival analysis over a 5-year
405 period. Cox proportional hazard analyses were performed to determine the prognostic value of CD155
406 overall methylation mean and CpG4-> CpG9 average methylation (sub_mean) in breast cancer patients.

407 Cox proportional hazard models were fit to estimate the effect of the non-dichotomized CD155 global
408 methylation mean and CpG4 -> CpG9 average methylation percentages, accounting for tissue type. A
409 significant association between CD155 global methylation mean or CpG4-> CpG9 average methylation and
410 overall survival could be confirmed. The trend towards a negative effect of methylation percentage on
411 patient survival was observed. In univariate Cox proportional hazard analysis, increased CD155 global
412 methylation mean percentage (Hazard ratio [HR] = 1.051, 95% confidence interval (CI) = 1.010 to 1.095, *p*-
413 value = 0.015) or sub_mean methylation percentage (HR = 1.044, 95% CI = 1.003 to 1.087, *p*-value = 0.033)
414 were significantly associated with reduced OS. Changes in DNA methylation at specific CpG sites showed
415 a significant correlation between increased methylation at CpG7 individual site and reduced overall
416 survival (HR = 1.049, 95% CI = 1.007 to 1.094, *p*-value = 0.023)

417 Multivariate Cox proportional hazard analyses including SBR grade, molecular group, tumor size, distant
418 metastasis, TILs and NK-TILs infiltration, and the expression of both cytoplasmic and membranous CD155
419 protein added significant prognostic information with regard to OS and DFS for CD155 global methylation
420 mean percentage (HR = 1.106, 95% CI = 1.038 to 1.177, *p*-value = 0.002 for OS ; HR = 1.064, 95% CI = 1.008
421 to 1.122, *p*-value = 0.024 for DFS) or CpG4 -> CpG9 average methylation percentage (HR = 1.097, 95% CI =
422 1.031 to 1.167, *p*-value = 0.003 for OS ; HR = 1.059, 95% CI = 1.004 to 1.116, *p*-value = 0.036 for DFS). These
423 results confirm that CD155 methylation is an independent predictor of survival.

424 Since CD155 mRNA expression and DNA methylation seem to be related, we next sought to determine
425 their value in predicting clinical outcome. Multivariate analysis further confirmed that CD155 methylation
426 is an independent risk factor for breast cancer patients. The impact of other covariates (adjustment
427 factors), including CD155 membranous mRNA isoform expression, SBR grade, molecular group, tumor size,
428 metastasis, TILs and NK-TILs infiltration, and the expression m-CD155 and cyt-CD155 protein on overall
429 survival and disease-free survival, was tested and showed a significant and unfavorable effect of CpG4->
430 CpG9 average methylation percentage (sub_mean) on survival (HR = 1.103, 95% CI = 1.024 to 1.187, *p*-
431 value = 0.010 for OS ; HR = 1.059, 95% CI = 1.001 to 1.121, *p*-value = 0.048 for DFS). Furthermore, the
432 prognostic value of CD155 membranous mRNA isoform expression on OS was also verified in the combined
433 analysis, and the results showed that lower expression pointed to poorest overall survival (HR = 0.874,
434 95% CI =0.712 to 1.074). In addition, the impacts of CD155 membranous mRNA isoform expression and m-
435 CD155 protein expression on patient's outcome are consistent (HR = 0.472, 95% CI =0.132 to 1.691).

436

437 **DISCUSSION**

438 Breast cancer is known to be one of the most complex, multi-factorial and multi-signal biological process
439 in carcinogenesis. Gene mutations and epigenetic modifications are factors resulting in tumorigenesis and
440 cancer progression of breast tumors. Besides, aberrant DNA methylation patterns are associated with
441 transcriptional repression, abnormal activation or inactivation of signaling pathways, abnormal apoptotic
442 mechanisms, activation of proto-oncogenes and the promotion of tumorigenesis. One of the most
443 attractive routes is the panel of immune checkpoint molecules which seems to have an important role in
444 the physiopathology of cancers. Among these molecules, CD155 expression has been recently described
445 with its pivotal function in a wide range of malignant cancers due to its complex interactions and
446 associated roles in the immune response [8]–[11], [14], [31]. More specifically, we have previously
447 reported the differential contribution of CD155 protein expression according to its localization site in
448 breast cancer progression and outcome. We provided evidence that CD155 is expressed at the cytoplasmic
449 or membranous level, thereby differential localization seems to have an importance in the tumor
450 microenvironment designing and physio-pathological features [14]. Interestingly, CD155 gene
451 transcription leads to mRNA products that can be alternatively spliced into different isoforms and
452 ultimately translated in four possible proteins, two transmembrane forms and two soluble forms [17]. For
453 this, we have hypothesized an epigenetic regulation, we precisely speculate changes in methylation status
454 of CD155 gene. In this study, we have evaluated the potential use of CD155 promoter methylation as a
455 prognostic biomarker in breast cancer. DNA methylation changes were validated by pyrosequencing, the
456 targeted region in our study contains 14 specific CpGs sites in the promoter region of CD155 gene.

457 We tempted to elucidate whether CD155 expression is under direct epigenetic control in breast cancer
458 patients. Indeed, transcriptional analyses were carried out in order to ascertain if hypomethylation
459 variations would affect CD155 mRNA expression. Our results showed consistent patterns where trends
460 were consistently negative for all CpG sites. Thus, we observed higher but not statistically significant CD155
461 membranous mRNA isoform transcription levels among samples lacking DNA methylation. Previously,
462 many studies have reported that gene expression is a complex process and that the interplay between
463 many different genetic, epigenetic, and epi-transcriptomic factors may also be involved in regulation of
464 gene expression [32]–[34]. Besides, differences in methylation levels might be necessary but not sufficient
465 for genes expression. Our data seem to point into the same direction; thus, this might explain the lack of
466 significative association between CD155 methylation and mRNA expression. Further, in order to clarify the
467 interplay between protein and mRNA expression, we aimed to confirm whether CD155 membranous

468 mRNA isoform expression is related to protein localization. Our results showed a positive association
469 between CD155 membranous mRNA isoform overexpression and high membranous CD155 (m-CD155)
470 protein localization. The consistency between CD155 mRNA isoform expression and protein localization
471 suggests that the expression of m-CD155 protein reflects the transcription of the corresponding isoform
472 and is likely to be regulated at the transcriptional level in breast cancer tissues. This conclusion is supported
473 by previous study showing the relationship between gene expression measured at the mRNA level and the
474 corresponding protein level in lung adenocarcinomas [35].

475 Our results identify for the first time that the CD155 promoter methylation pattern is a reliable
476 clinicopathological biomarker of immune checkpoint regulation in solid tumors. Previous studies have only
477 shown the expression of CD155 by cancer cells but no study has reported its promoter methylation status.
478 Herein we have initially described the clinical impact of CD155 promoter methylation pattern. Statistical
479 analyses demonstrated that higher levels of CD155 promoter methylation correlated with higher tumor
480 size. In agreement with this observation, previous studies reported that CD155 expression level was
481 significantly associated with tumor size in breast cancer, soft tissue sarcoma and in primary small cell
482 carcinoma of the esophagus [36]–[38]. Further, CD155 methylation levels among molecular subgroups
483 showed significant results, most importantly, the Her2, LB and TNBC groups correlated with higher
484 methylation rates. In contrast, recent studies reported that the proportion of patients with CD155
485 expression was higher in TNBC compared to LA groups [15], [39]. Our conclusion does not differ from
486 previous reports as methylation rates in our study remain relatively low. In addition, we identified a strong
487 and positive correlation between a higher methylation percentage and the expression of the HER2
488 receptor. Meanwhile, negative correlations with progesterone and estrogen receptors expression status
489 were identified. Thus, on the basis of data obtained from the publicly available database from The Cancer
490 Genome Atlas (TCGA), we compared clinical DNA methylation data from the TCGA with differentially
491 methylated DNA within the targeted CpG motifs in CD155 gene promoter, and we obtained similar
492 conclusions. In fact, CD155 expression and its promoter methylation status are negatively correlated,
493 which is confirmed by the Pearson correlation coefficients. Besides, a comprehensive study by the TCGA
494 Network [40], [41], have demonstrated clear differences in CD155 expression and methylation, as well as
495 HER2, estrogen and progesterone receptor status, and molecular subtypes between the different breast
496 cancer samples.

497 Moreover, when comparing patient's distant metastasis and lymphovascular invasion according to CD155
498 promoter methylation or protein expression in breast cancer tissues, data show a limited significant but

499 interesting association between no distant metastasis or lymphovascular invasion and CD155 promoter
500 methylation and with loss of m-CD155 protein expression in breast cancer tissues as we previously
501 reported [14]. Our results clearly show that CD155 promoter methylation correlated with CD155 protein
502 expression and the invasion process implying that methylation of the CD155 promoter may affect tumor
503 progression in advanced breast cancer tissues via the regulation of protein expression at the membranous
504 localization. This may be due to changes in the tumor microenvironment resulting from CD155 aberrant
505 methylation. Further studies investigating the mechanism behind this process may offer insights into
506 potential therapeutic targets or prognostic biomarkers in breast cancer disease monitoring. Indeed,
507 checkpoint inhibitors have become an efficient way for cancer therapy. Notably, monoclonal antibodies
508 targeting the PD-1/PD-L1 signaling axis have shown striking clinical success against multiple malignancies.
509 However, while these therapies are very efficient in certain tumors, others showed low response rates to
510 PD-1/PD-L1 blockade [42]. This discrepancy might be explained by the immune infiltrate, the differential
511 expression status of target molecules, and the impact of the tumor microenvironment. Interestingly,
512 CD155, which interacts with receptors expressed on T and NK cells, recently emerged as a compelling
513 immunotherapeutic target [43], [44]. CD155 has an immunoregulatory potential upon interaction with
514 DNAM-1, CD96, and TIGIT, resulting in two distinct profiles of effector cell activation. In the setting of
515 cancer, TIGIT is under active investigation as a target for immune checkpoint blockade owing to its
516 inhibitory effects on T cell proliferation and function [45]. In preclinical models, it was recently reported
517 that TIGIT blockade has limited efficacy as a monotherapy but is able to significantly potentiate the efficacy
518 of PD-1 and CD96 blockade [46]. It was demonstrated that TIGIT/PD-1 is expressed on CD8+ lymphocytes,
519 suggesting that cancerous cells may be able to upregulate PD-L1 and CD155 during immune evasion, by
520 interacting with their ligands expressed on TILs to suppress their cytotoxic activities. Additionally, CD155
521 overexpression on malignant epithelium in high-grade serous ovarian cancer suggests that the disease
522 may be subject to therapeutic strategies targeting CD155, such as oncolytic poliovirus, which is showing
523 promising results in phase I trials against malignant glioma [43]. Finally, it was demonstrated that
524 CD155/PVR is commonly expressed in TILs negative tumors suggesting that targeting the CD155/TIGIT
525 pathway might prove complementary to PD-1/PD-L1-directed approaches [46]. The deeper mechanisms
526 underlying this relationship deserves further exploration, and more particularly the significance of CD155
527 promotor methylation status in immunotherapy.

528 To further evaluate CD155 influence upon patient prognosis, multivariate analyses were conducted and
529 showed that decreased CD155 methylation mean percentage is significantly associated with better
530 patients' survival, which clearly reflects an unfavorable prognosis of CD155 methylation. It has been largely

531 demonstrated that CD155 has a pivotal role in a broad range of malignant tumors. A recent study reported
532 that overexpression of CD155 in cancer cells correlated with an unfavorable prognosis of patients with
533 lung adenocarcinoma [31], another study demonstrated that patients with pancreatic cancer displaying
534 higher CD155 expression levels had significantly poor prognosis [11]. Likewise, upregulated CD155
535 expression correlated with aggressive clinical-pathological features and unfavorable prognosis in patients
536 with Cholangiocarcinoma [47] and with Primary Small Cell Carcinoma of the Esophagus [38]. While these
537 previous studies reported that CD155 expression was a poor prognostic marker, other studies reported
538 opposite results. Thus, studies on breast carcinoma and hepatocellular carcinoma showed that tumors
539 overexpressing CD155 correlated with good prognosis [14], [48]. These discrepancies suggest that CD155
540 may serve dual functions owing to its immunological and non-immunological mechanisms in various types
541 of human cancers. Our finding is in good agreement with previous studies showing that the expression of
542 CD155 is positively correlated with good prognosis in breast cancer and hepatocellular carcinoma [14],
543 [48]. Our results showed consistency with m-CD155 protein expression findings and further elucidated
544 that CD155 methylation is an independent predictor of prognosis. With the analysis above, we believe that
545 CD155 methylation may be a prospective biomarker to predict the prognosis of breast cancer patients.
546 Taken together, we speculate CD155 methylation as a potential regulator of CD155 expression and as an
547 independent predictor of overall survival and disease-free survival in breast cancer patients.

548 **CONCLUSION**

549 Data generated in our study provide more evidence in respect to the identification of new reliable
550 epigenetic biomarkers which is important in achieving a better prognosis. To date, CD155 immune
551 checkpoint methylation has not been analyzed in breast cancer or any type of cancer. Our study suggests
552 that quantification of CD155 promoter methylation levels by pyrosequencing is a promising diagnostic
553 biomarker assay approach to predict breast tumor evolution and prognosis. Specifically, we identified six
554 CpGs sites in CD155 gene promoter which perform well compared to the global methylation of all 14 CpGs.
555 Hence, combining CD155 CpG4 -> CpG9 methylation rates could improve its sensitivity to correlate with
556 clinical-pathological parameters and disease outcome. One of the intriguing findings of our study is that
557 single CpG site 7 showed significant correlations with NK cell infiltrate, clinical parameters and prognosis.
558 The level of methylation at this site deserves confirmation for therapeutic approaches as a potential target.
559 Thus, further research on the role of CD155 methylation would be of considerable interest and will
560 certainly add to our understanding of the regulation of gene products.

561

562 **ACKNOWLEDGEMENTS**

563 We thank our study participants for their contribution to this study. A further thanks goes to the Protein
564 Chemistry, Proteomics and Epigenetic Signaling (PPES), University of Antwerp, team members for their
565 collaboration and valuable contribution. This work was partially supported by ISESCO (Islamic Educational,
566 Scientific and Cultural Organization) Research grant (Ref No. 2148).

567 **REFERENCES**

568 [1] D. M. Pardoll, "The blockade of immune checkpoints in cancer immunotherapy," *Nat. Rev. Cancer*,
569 vol. 12, no. 4, pp. 252–264, Mar. 2012, doi: 10.1038/nrc3239.
570 [2] S. L. Topalian, C. G. Drake, and D. M. Pardoll, "Immune checkpoint blockade: a common denominator
571 approach to cancer therapy," *Cancer Cell*, vol. 27, no. 4, pp. 450–461, Apr. 2015, doi:
572 10.1016/j.ccell.2015.03.001.
573 [3] P. Sharma and J. P. Allison, "The future of immune checkpoint therapy," *Science*, vol. 348, no. 6230,
574 pp. 56–61, Apr. 2015, doi: 10.1126/science.aaa8172.
575 [4] B. Chaudhary and E. Elkord, "Regulatory T Cells in the Tumor Microenvironment and Cancer
576 Progression: Role and Therapeutic Targeting," *Vaccines (Basel)*, vol. 4, no. 3, Aug. 2016, doi:
577 10.3390/vaccines4030028.
578 [5] V. Sasidharan Nair and E. Elkord, "Immune checkpoint inhibitors in cancer therapy: a focus on T-
579 regulatory cells," *Immunol. Cell Biol.*, vol. 96, no. 1, pp. 21–33, 2018, doi: 10.1111/imcb.1003.
580 [6] W. C. Dougall, S. Kurtulus, M. J. Smyth, and A. C. Anderson, "TIGIT and CD96: new checkpoint
581 receptor targets for cancer immunotherapy," *Immunol. Rev.*, vol. 276, no. 1, pp. 112–120, 2017, doi:
582 10.1111/imr.12518.
583 [7] C. J. Chan *et al.*, "The receptors CD96 and CD226 oppose each other in the regulation of natural killer
584 cell functions," *Nat. Immunol.*, vol. 15, no. 5, pp. 431–438, May 2014, doi: 10.1038/ni.2850.
585 [8] D. Masson *et al.*, "Overexpression of the CD155 gene in human colorectal carcinoma," *Gut*, vol. 49,
586 no. 2, pp. 236–240, Aug. 2001.
587 [9] R. Nakai *et al.*, "Overexpression of Necl-5 correlates with unfavorable prognosis in patients with lung
588 adenocarcinoma," *Cancer Sci.*, vol. 101, no. 5, pp. 1326–1330, May 2010, doi: 10.1111/j.1349-
589 7006.2010.01530.x.
590 [10] V. Bevelacqua *et al.*, "Nectin like-5 overexpression correlates with the malignant phenotype in
591 cutaneous melanoma," *Oncotarget*, vol. 3, no. 8, pp. 882–892, Aug. 2012, doi:
592 10.18632/oncotarget.594.
593 [11] S. Nishiwada *et al.*, "Clinical significance of CD155 expression in human pancreatic cancer,"
594 *Anticancer Res.*, vol. 35, no. 4, pp. 2287–2297, Apr. 2015.
595 [12] K. E. Sloan, J. K. Stewart, A. F. Treloar, R. T. Matthews, and D. G. Jay, "CD155/PVR enhances glioma
596 cell dispersal by regulating adhesion signaling and focal adhesion dynamics," *Cancer Res.*, vol. 65, no.
597 23, pp. 10930–10937, Dec. 2005, doi: 10.1158/0008-5472.CAN-05-1890.
598 [13] H. Stamm *et al.*, "Targeting the TIGIT-PVR immune checkpoint axis as novel therapeutic option in
599 breast cancer," *Oncoimmunology*, vol. 8, no. 12, p. e1674605, 2019, doi:
600 10.1080/2162402X.2019.1674605.
601 [14] H. Triki *et al.*, "CD155 expression in human breast cancer: Clinical significance and relevance to
602 natural killer cell infiltration," *Life Sciences*, vol. 231, p. 116543, Aug. 2019, doi:
603 10.1016/j.lfs.2019.116543.
604 [15] Y.-C. Li *et al.*, "Overexpression of an Immune Checkpoint (CD155) in Breast Cancer Associated with
605 Prognostic Significance and Exhausted Tumor-Infiltrating Lymphocytes: A Cohort Study," *Journal of*

606 *Immunology Research*, 2020. https://www.hindawi.com/journals/jir/2020/3948928/ (accessed Apr.
607 08, 2020).
608 [16] K. J. D. A. Excoffon, J. R. Bowers, and P. Sharma, "1. Alternative splicing of viral receptors: A review
609 of the diverse morphologies and physiologies of adenoviral receptors," *Recent Res Dev Virol*, vol. 9,
610 pp. 1–24, 2014.
611 [17] S. Koike *et al.*, "The poliovirus receptor protein is produced both as membrane-bound and secreted
612 forms," *EMBO J.*, vol. 9, no. 10, pp. 3217–3224, Oct. 1990.
613 [18] B. B *et al.*, "Identification of secreted CD155 isoforms.," *Biochem Biophys Res Commun*, vol. 309, no.
614 1, pp. 175–182, Sep. 2003, doi: 10.1016/s0006-291x(03)01560-2.
615 [19] E. Lozano, M. Dominguez-Villar, V. Kuchroo, and D. A. Hafler, "The TIGIT/CD226 axis regulates human
616 T cell function," *J. Immunol.*, vol. 188, no. 8, pp. 3869–3875, Apr. 2012, doi:
617 10.4049/jimmunol.1103627.
618 [20] M. Kulis and M. Esteller, "DNA methylation and cancer," *Adv. Genet.*, vol. 70, pp. 27–56, 2010, doi:
619 10.1016/B978-0-12-380866-0.60002-2.
620 [21] N. Sinčić and Z. Herceg, "DNA methylation and cancer: ghosts and angels above the genes," *Curr Opin*
621 *Oncol*, vol. 23, no. 1, pp. 69–76, Jan. 2011, doi: 10.1097/CCO.0b013e3283412eb4.
622 [22] Y. Wu, M. Sarkissyan, and J. V. Vadgama, "Epigenetics in breast and prostate cancer," *Methods Mol.*
623 *Biol.*, vol. 1238, pp. 425–466, 2015, doi: 10.1007/978-1-4939-1804-1_23.
624 [23] V. Sasidharan Nair, H. El Salhat, R. Z. Taha, A. John, B. R. Ali, and E. Elkord, "DNA methylation and
625 repressive H3K9 and H3K27 trimethylation in the promoter regions of PD-1, CTLA-4, TIM-3, LAG-3,
626 TIGIT, and PD-L1 genes in human primary breast cancer," *Clin Epigenetics*, vol. 10, p. 78, 2018, doi:
627 10.1186/s13148-018-0512-1.
628 [24] D. Roulois, H. L. Yau, and D. D. De Carvalho, "Pharmacological DNA demethylation: Implications for
629 cancer immunotherapy," *Oncoimmunology*, vol. 5, no. 3, p. e1090077, Mar. 2016, doi:
630 10.1080/2162402X.2015.1090077.
631 [25] P. Maruvada, W. Wang, P. D. Wagner, and S. Srivastava, "Biomarkers in molecular medicine: cancer
632 detection and diagnosis," *BioTechniques*, vol. Suppl, pp. 9–15, Apr. 2005, doi: 10.2144/05384su04.
633 [26] A. C. Wolff *et al.*, "Recommendations for human epidermal growth factor receptor 2 testing in breast
634 cancer: American Society of Clinical Oncology/College of American Pathologists clinical practice
635 guideline update," *J. Clin. Oncol.*, vol. 31, no. 31, pp. 3997–4013, Nov. 2013, doi:
636 10.1200/JCO.2013.50.9984.
637 [27] L. Bouzidi *et al.*, "Prognostic value of natural killer cells besides tumor infiltrating lymphocytes in
638 breast cancer tissues," *Clinical Breast Cancer*, Feb. 2021, doi: 10.1016/j.clbc.2021.02.003.
639 [28] S. J and R. Dw, "Purification of nucleic acids by extraction with phenol:chloroform.," *CSH Protoc*, vol.
640 2006, no. 1, pp. 169–170, Jun. 2006, doi: 10.1101/pdb.prot4455.
641 [29] R. K. Saiki *et al.*, "Primer-directed enzymatic amplification of DNA with a thermostable DNA
642 polymerase," *Science*, vol. 239, no. 4839, pp. 487–491, Jan. 1988.
643 [30] K. Declerck *et al.*, "Interaction between prenatal pesticide exposure and a common polymorphism
644 in the PON1 gene on DNA methylation in genes associated with cardio-metabolic disease risk—an
645 exploratory study," *Clin Epigenetics*, vol. 9, Apr. 2017, doi: 10.1186/s13148-017-0336-4.
646 [31] Y. Sun *et al.*, "Combined evaluation of the expression status of CD155 and TIGIT plays an important
647 role in the prognosis of LUAD (lung adenocarcinoma)," *Int. Immunopharmacol.*, vol. 80, p. 106198,
648 Jan. 2020, doi: 10.1016/j.intimp.2020.106198.
649 [32] P. A. Jones and S. B. Baylin, "The epigenomics of cancer," *Cell*, vol. 128, no. 4, pp. 683–692, Feb. 2007,
650 doi: 10.1016/j.cell.2007.01.029.
651 [33] P. A. Jones, "Functions of DNA methylation: islands, start sites, gene bodies and beyond," *Nat Rev*
652 *Genet*, vol. 13, no. 7, pp. 484–492, May 2012, doi: 10.1038/nrg3230.

[34] E. R. Gibney and C. M. Nolan, “Epigenetics and gene expression,” *Heredity*, vol. 105, no. 1, Art. no. 1, Jul. 2010, doi: 10.1038/hdy.2010.54.

[35] G. Chen *et al.*, “Discordant Protein and mRNA Expression in Lung Adenocarcinomas *,” *Molecular & Cellular Proteomics*, vol. 1, no. 4, pp. 304–313, Apr. 2002, doi: 10.1074/mcp.M200008-MCP200.

[36] H. Yong *et al.*, “CD155 expression and its prognostic value in postoperative patients with breast cancer,” *Biomedicine & Pharmacotherapy*, vol. 115, p. 108884, Jul. 2019, doi: 10.1016/j.biopha.2019.108884.

[37] S. Atsumi, A. Matsumine, H. Toyoda, R. Niimi, T. Iino, and A. Sudo, “Prognostic significance of CD155 mRNA expression in soft tissue sarcomas,” *Oncol Lett*, vol. 5, no. 6, pp. 1771–1776, Jun. 2013, doi: 10.3892/ol.2013.1280.

[38] K. Zhao, L. Ma, L. Feng, Z. Huang, X. Meng, and J. Yu, “CD155 Overexpression Correlates With Poor Prognosis in Primary Small Cell Carcinoma of the Esophagus,” *Front. Mol. Biosci.*, vol. 7, 2021, doi: 10.3389/fmolb.2020.608404.

[39] R.-B. Wang *et al.*, “Overexpression of CD155 is associated with PD-1 and PD-L1 expression on immune cells, rather than tumor cells in the breast cancer microenvironment,” *World J Clin Cases*, vol. 8, no. 23, pp. 5935–5943, Dec. 2020, doi: 10.12998/wjcc.v8.i23.5935.

[40] “The Cancer Genome Atlas Program - National Cancer Institute,” Jun. 13, 2018. https://www.cancer.gov/about-nci/organization/ccg/research/structural-genomics/tcga (accessed Feb. 20, 2021).

[41] A. Koch, T. De Meyer, J. Jeschke, and W. Van Criekinge, “MEXPRESS: visualizing expression, DNA methylation and clinical TCGA data,” *BMC Genomics*, vol. 16, p. 636, Aug. 2015, doi: 10.1186/s12864-015-1847-z.

[42] J. S. O’Donnell, G. V. Long, R. A. Scolyer, M. W. L. Teng, and M. J. Smyth, “Resistance to PD1/PDL1 checkpoint inhibition,” *Cancer Treatment Reviews*, vol. 52, pp. 71–81, Jan. 2017, doi: 10.1016/j.ctrv.2016.11.007.

[43] J. S. O’Donnell, J. Madore, X.-Y. Li, and M. J. Smyth, “Tumor intrinsic and extrinsic immune functions of CD155,” *Semin Cancer Biol*, vol. 65, pp. 189–196, Oct. 2020, doi: 10.1016/j.semcancer.2019.11.013.

[44] K. B. Lupo and S. Matosevic, “CD155 immunoregulation as a target for natural killer cell immunotherapy in glioblastoma,” *Journal of Hematology & Oncology*, vol. 13, no. 1, p. 76, Jun. 2020, doi: 10.1186/s13045-020-00913-2.

[45] J.-M. Chauvin *et al.*, “TIGIT and PD-1 impair tumor antigen–specific $CD8^+$ T cells in melanoma patients,” *J Clin Invest*, vol. 125, no. 5, pp. 2046–2058, May 2015, doi: 10.1172/JCI80445.

[46] J. Smazynski *et al.*, “The immune suppressive factors CD155 and PD-L1 show contrasting expression patterns and immune correlates in ovarian and other cancers,” *Gynecologic Oncology*, vol. 158, no. 1, pp. 167–177, Jul. 2020, doi: 10.1016/j.ygyno.2020.04.689.

[47] D.-W. Huang, M. Huang, X.-S. Lin, and Q. Huang, “CD155 expression and its correlation with clinicopathologic characteristics, angiogenesis, and prognosis in human cholangiocarcinoma,” *Onco Targets Ther*, vol. 10, pp. 3817–3825, 2017, doi: 10.2147/OTT.S141476.

[48] P. Qu *et al.*, “Loss of CD155 expression predicts poor prognosis in hepatocellular carcinoma,” *Histopathology*, vol. 66, no. 5, pp. 706–714, Apr. 2015, doi: 10.1111/his.12584.

697 **FIGURE LEGENDS**

698 **Figure 1: Schematic representation of the human CD155 gene with its promoter region and selected CpG**
699 **Island.** The studied 14 CpG sites are shown as lollypops within the promoter range.
700

701 **Figure 2: CD155 promoter methylation mean according to clinical pathological features.** The x-axis shows
702 the mean percentage of global methylation and y-axis shows **(a)** SBR grade, **(b)** Tumor size, **(c)** Molecular
703 group, **(d)** Her2 receptor, **(e)** RE receptor, **(f)** RP receptor.
704
705
706 **Figure 3: CD155 promoter methylation percentage of individual CpGs sites according to NK-TILs.** The x-
707 axis shows the methylation percentage of **(a)** CpG7, **(b)** CpG8, **(c)** CpG9 and **(d)** CpG11 sites and y-axis
708 shows NK-TILs.
709

710 **Figure 4: Different DNA methylation patterns for CD155 with respect to transcription levels (a)**
711 Distribution of methylation mean percentage across six CpG sites and **(b)** methylation dichotomized
712 according to its median into highly or weakly hypomethylated tumors according to CD155 membranous
713 mRNA isoform expression ($2^{\Delta\Delta Cq}$).

714

715 **Figure 5: Correlations between CD155 membranous mRNA isoform expression analyzed by RT-qPCR and**
716 **protein localization determined by IHC**. Boxplot representation showing a comparison of **(a)** m-CD155
717 and **(b)** cyt-CD155 distribution with respect to CD155 membranous isoform transcription levels ($2^{\Delta\Delta Cq}$).
718

719

720

721

722

723

724

725

726

727

728

729

730

731 Table 1: Sequences and amplicon size of primers used for CD155 pyrosequencing.

Gene	PCR primers	Product length	Sequencing primer
CD155	5’-ATTTGGAATGTGGGAGATTTTATATAGGAA-3’ 5’-BIOTIN-AAACCACCCAAACTAACCC-3’	142 bp	5’-GAAGTAGTTTTTTTTAGTGGGTA-3’

732

733

734

735

736

737

738

739

740

741

742

743

744

745

746

747

748

749

750

751

752

753 Table 2: Associations of CD155 promotor methylation (overall mean methylation or sub_mean methylation
754 values) and CD155 mRNA expression (normalized counts) with clinical-pathological and immunological
755 parameters.

Variable	N (%)	*Mean Methylation*				*Sub_mean Methylation*				*mRNA expression ($2^{\Delta\Delta Cq}$)*			
		Mean ± SD	Min	Max	*p*-value	Mean ± SD	Min	Max	*p*-value	Mean ± SD	Min	Max	*p*-value
Age					0.191				2.46E-01				0.707
≤40	18.1	3.5±4.6	0.19	19.41		3.58±6.06	0	24.68		2.47±5.5	0.05	25.29	
>40	81.9	4.01±6.27	0.62	40.56		4±6.82	0.51	40.38		2.18±2.92	0.007	15.84	
Menauposal Status					0.545				5.67e- 1				0.858
Menauposed	52.6	4.25±6.9	0.62	40.56		4.2±7.5	0.51	40.38		2.2±2.9	0.013	15.84	
Premenauposed	47.4	3.63±4.81	0.19	23.67		3.6±5.7	0	24.68		2.3±4.2	0.007	25.29	
SBR					0.064				5.84E-02				0.207
I	18.1	1.55±0.5	0.54	2.7		1.34±0.39	0.51	2.16		1.35±1.27	0.02	4.34	
II	37.9	3.96±5.35	0.19	29.23		3.95±6.04	0	27.6		3.05±4.9	0.02	25.29	
III	44	4.91±7.34	0.69	40.56		4.94±8.16	0.62	40.38		1.97±2.78	0.007	15.84	
GM					**0.003**				**0.0001**				0.787
LA	25.9	1.63±0.67	0.54	3.3		1.37±0.43	0.66	2.16		1.95±2.62	0.02	11.39	
LB	12.9	5.75±6.98	1.03	29.23		5.67±7	0.83	27.6		2.96±6.87	0.007	25.29	
LB-Like	32.8	2.8±3.44	0.19	19.41		2.25±3.15	0	19.19		2.48±3.23	0.03	15.48	
HER2	11.2	7.2±6.89	1.58	19.44		8.94±9.92	1.26	26.11		1.01±1.37	0.02	4.3	
TNBC	17.2	6.06±9.59	0.74	40.56		6.2±9.87	0.74	40.38		2.22±2.39	0.04	7.16	
Histological type					0.631				6.53E-01				**0.045**
CCI	80.2	3.25±5.77	0.19	40.56		3.79±6.47	0	40.38		1.86±3.33	0.007	25.29	
Others	19.8	4.44±6.79	0.62	29.23		4.39±746	0.51	27.6		3.66±4.08	0.04	15.84	
Lymphovacular invasion					0.228				2.14E-01				0.612
No	59.5	3.44±5.95	0.19	40.56		3.38±6.4	0	40.38		2.38±3.73	0.007	25.29	
Yes	40.5	4.75±5.98	0.62	29.23		4.75±7.02	0.51	27.6		2±3.28	0.013	15.84	
ER expression					**0.007**				**7.58E-04**				0.128
Negative	33.6	5.82±8.12	0.74	40.56		6.42±9.4	0.74	40.38		3.09±5.33	0.02	25.29	
Positive	66.4	2.96±4.16	0.19	29.23		2.59±4.07	0	27.6		1.87±2.4	0.007	11.39	
PR expression					**0.0302**				**5.03E-03**				0.846
Negative	41.4	5.24±7.47	0.19	40.56		5.67±8.66	0	40.38		2.33±3.38	0.019	15.84	
Positive	58.6	2.99±4.38	0.54	29.23		2.62±4.28	0.51	27.6		2.18±3.68	0.007	25.29	
Her2 expression					**0.0052**				**5.58E-04**				0.939
Negative	75.9	3.16±5.42	0.19	40.56		2.87±5.52	0	40.38		2.25±2.89	0.02	15.84	
Positive	24.1	6.46±6.98	1.03	29.23		7.25±8.69	0.83	27.6		2.19±5.47	0.007	25.29	
Tumor size					**0.001**				**3.75E-04**				0.56
T1 ≤ 2 cm	19.8	3.9±5.18	0.8	23.67		3.87±6.31	0.66	24.64		2.91±5.29	0.019	25.29	
2 < T2 ≤ 5 cm	55.2	2.85±3.19	0.19	19.41		2.63±3.55	0	19.19		1.82±2.7	0.007	11.39	
T3 > 5 cm	11.2	3.32±4.42	0.54	17.76		3.57±5.72	0.73	22.45		3.15±4.42	0.06	15.84	
T4	13.8	8.76±11.55	0.72	40.56		9.26±12.27	0.66	40.38		2.22±2.3	0.06	7.95	

Lymphnode status					0.79				4.52E-01				0.68
N0	44	4.03±7.07	0.54	40.56		3.86±7.44	0.51	40.38		2.56±4.33	0.007	25.29	
N1	31	3.69±5.18	0.19	29.23		3.45±5.27	0	27.6		1.78±2.07	0.01	7.95	
N2	17.2	3.42±4.69	0.72	17.76		3.55±6.14	0.66	22.45		2.39±3.41	0.02	11.39	
N3	7.8	5.62±4.43	0.93	14.85		6.79±7.46	0.7	24.68		0.93±1.07	0.05	2.72	
Metastasis					0.0969				6.88E-02				0.378
M0	88.6	3.52±5.54	0.19	40.56		3.35±6.02	0	40.37		2.34±3.72	0.007	25.29	
M1	11.4	6.21±8.06	0.93	29.23		6.34±8.55	0.7	27.6		1.28±1.45	0.02	4.63	
TNM stage					0.264				1.41E-01				0.75
I	14.9	3.36±5.36	0.8	23.67		2.96±5.1	0.66	22.49		3.22±5.81	0.09	25.29	
IIA	26.3	3.09±3.65	0.62	19.41		2.75±3.83	0.51	19.19		1.73±2.34	0.007	7.56	
IIB	21.9	2.86±3.12	0.19	14.17		2.75±3.71	0	17.13		2.15±3.51	0.01	15.84	
IIIA	13.2	3.08±3.99	0.77	17.76		3.02±5.21	0.88	22.45		3.07±3.75	0.02	11.39	
IIIB	9.7	6.76±11.85	0.72	40.56		7.1±12.7	0.66	40.38		2.24±4.42	0.06	7.95	
IIIC	2.6	3.95±1.68	1.62	5.56		3.98±2.63	1.38	7.59		0.2±0	0.2	0.2	
IV	11.4	6.21±8.06	0.93	29.23		6.34±8.55	0.7	27.6		1.28±1.45	0.02	4.63	
NK-TILs					0.081				0.0682				0.719
High	78.8	3.25±5.38	0.19	40.56		3.1±5.9	0	40.38		2.3±3.97	0.028	25.29	
Low	21.2	3.32±6.38	0.77	23.67		5.42±6.94	0.88	22.49		1.94±2.19	0.007	6.17	
TILs					0.596				8.63E-01				0.765
Low	53.5	3.45±4.95	0.54	29.23		3.47±5.56	0.51	27.6		2.67±4.4	0.02	25.29	
Moderate	28.1	4.65±7.7	0.62	40.56		4.05±7.6	0.7	40.38		1.81±2.56	0.007	10.67	
High	18.4	3.83±5.3	0.19	19.44		4.05±6.63	0	26.11		1.79±1.82	0.09	5.49	

Bold numbers indicate statistically significant correlations with *p*-values less than 0.05.

FIGURE 1

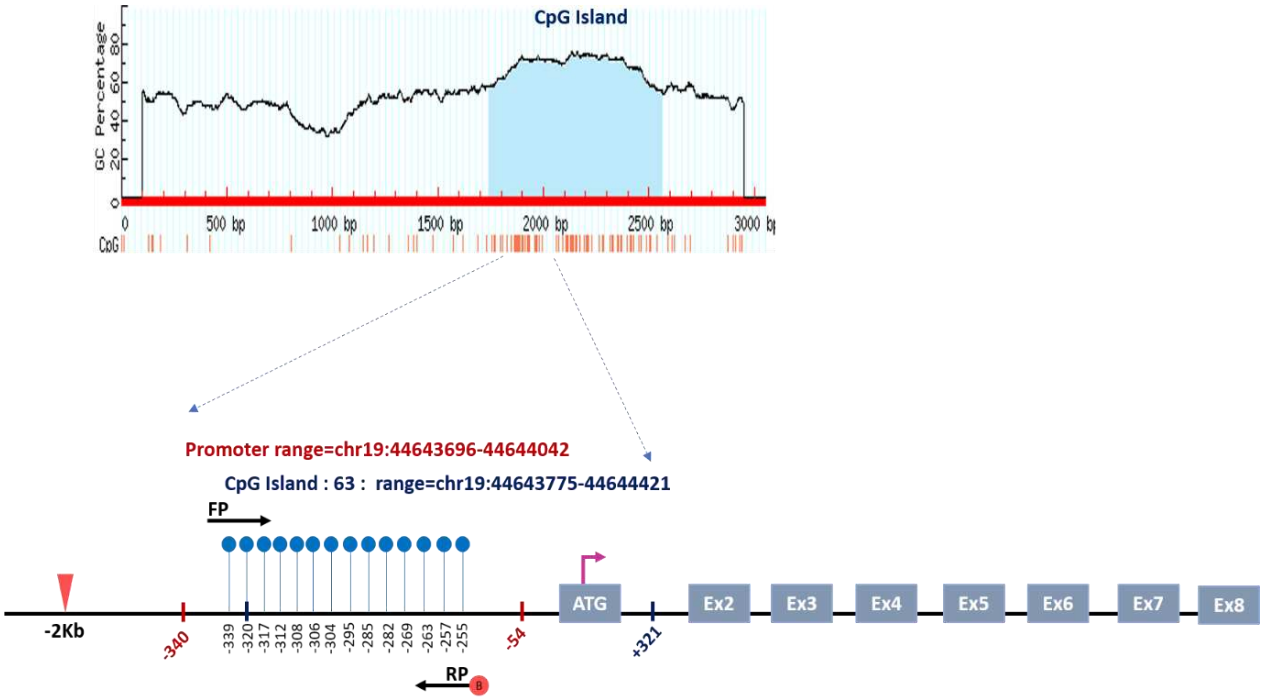
CpG Island
GC Percentage
0
20
40
60
80
0
500 bp
1000 bp
1500 bp
2000 bp
2500 bp
3000 bp
CpG
Promoter range=chr19:44643696-44644042
CpG Island : 63 : range=chr19:44643775-44644421
FP
-2Kb
-340
-339
-320
-317
-312
-308
-306
-304
-295
-285
-282
-269
-263
-257
-255
-54
ATG
+321
Ex2
Ex3
Ex4
Ex5
Ex6
Ex7
Ex8
RP

FIGURE 2

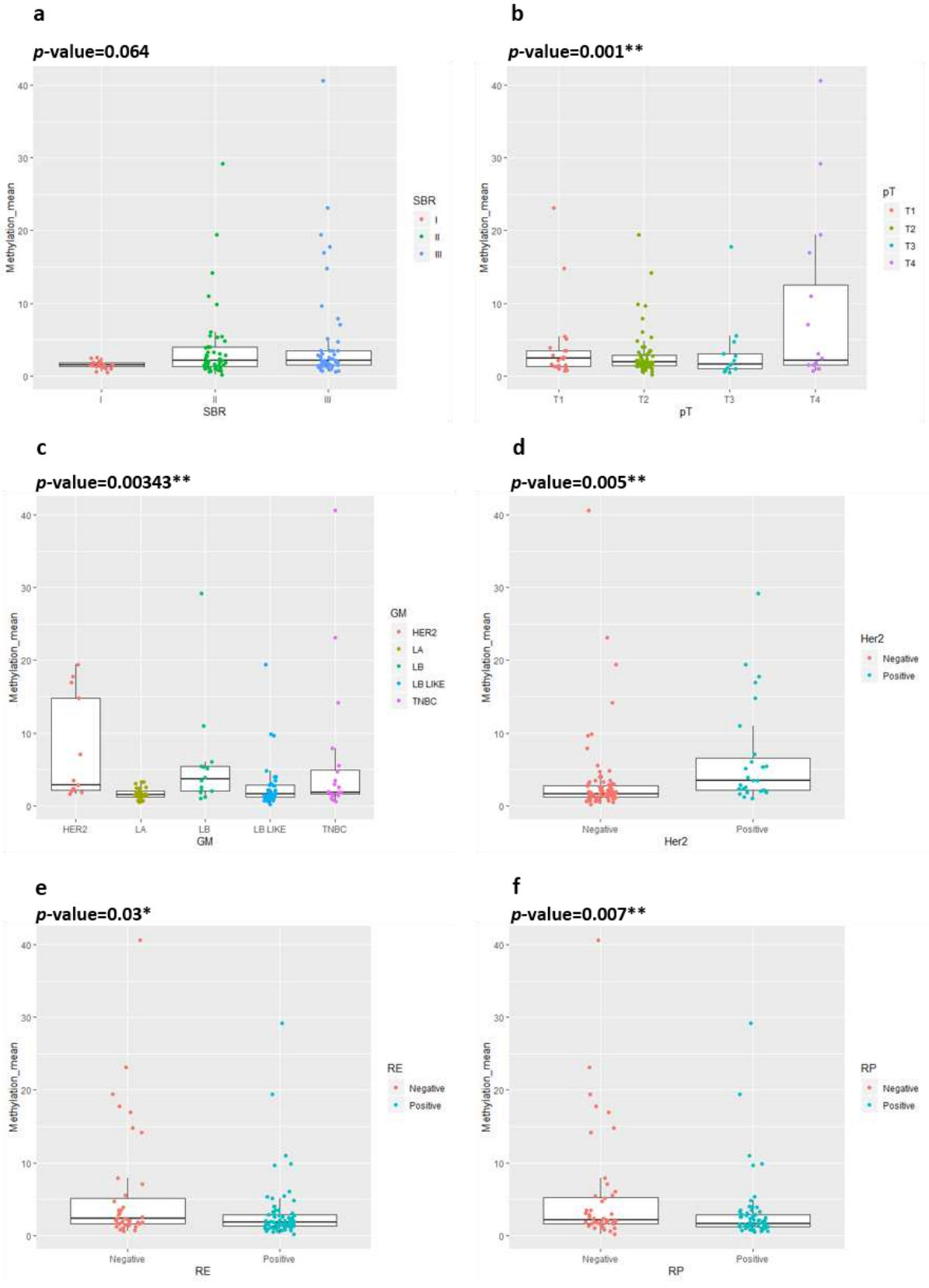
a
p-value=0.064
Methylation_mean
SBR
I
II
III
b
p-value=0.001**
Methylation_mean
pT
T1
T2
T3
T4
c
p-value=0.00343**
Methylation_mean
GM
HER2
LA
LB
LB LIKE
TNBC
d
p-value=0.005**
Methylation_mean
Her2
Negative
Positive
e
p-value=0.03*
Methylation_mean
RE
Negative
Positive
f
p-value=0.007**
Methylation_mean
RP
Negative
Positive

786 FIGURE 3

787

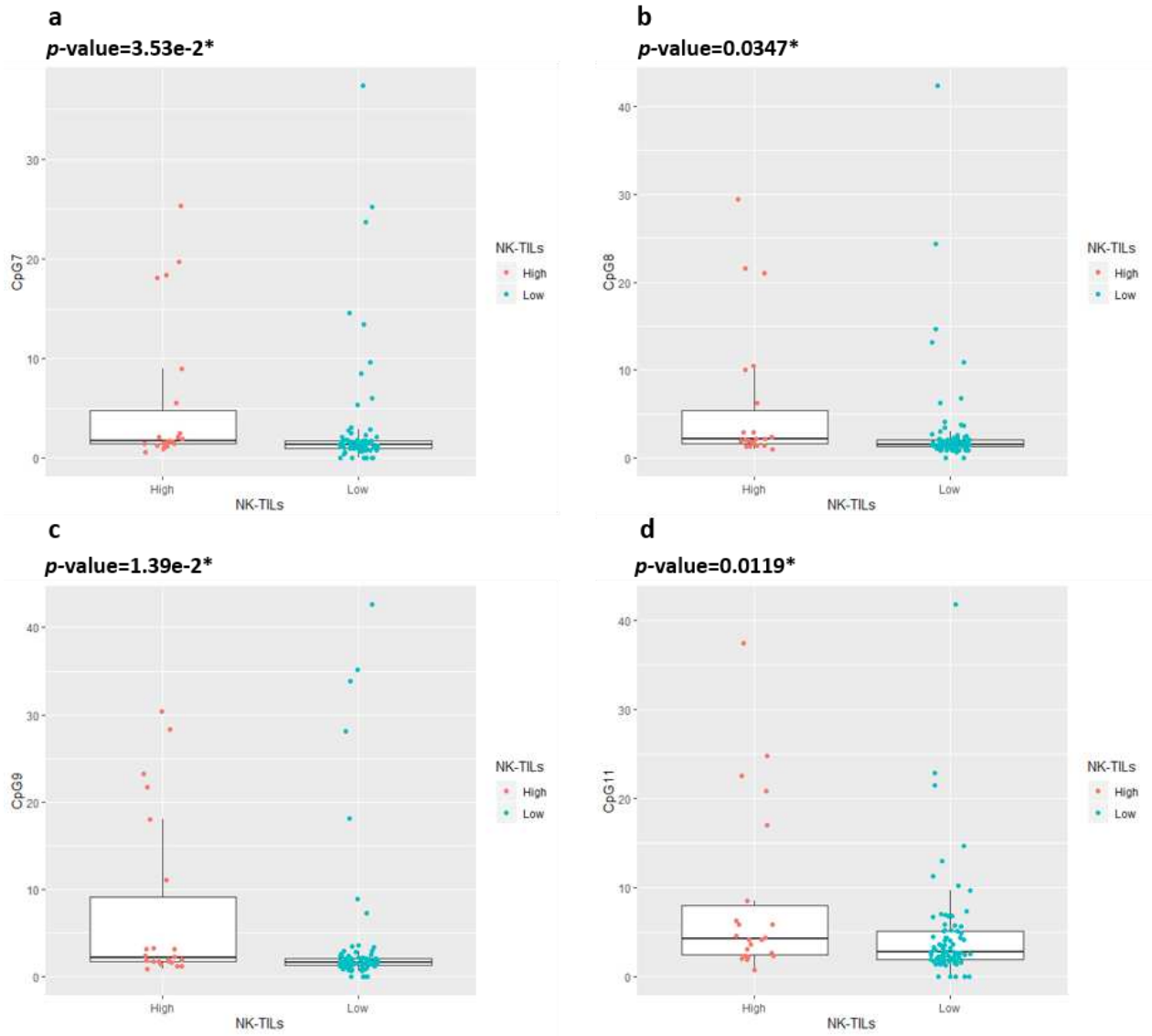

788
789

790

791

792

793

794

795

FIGURE 4

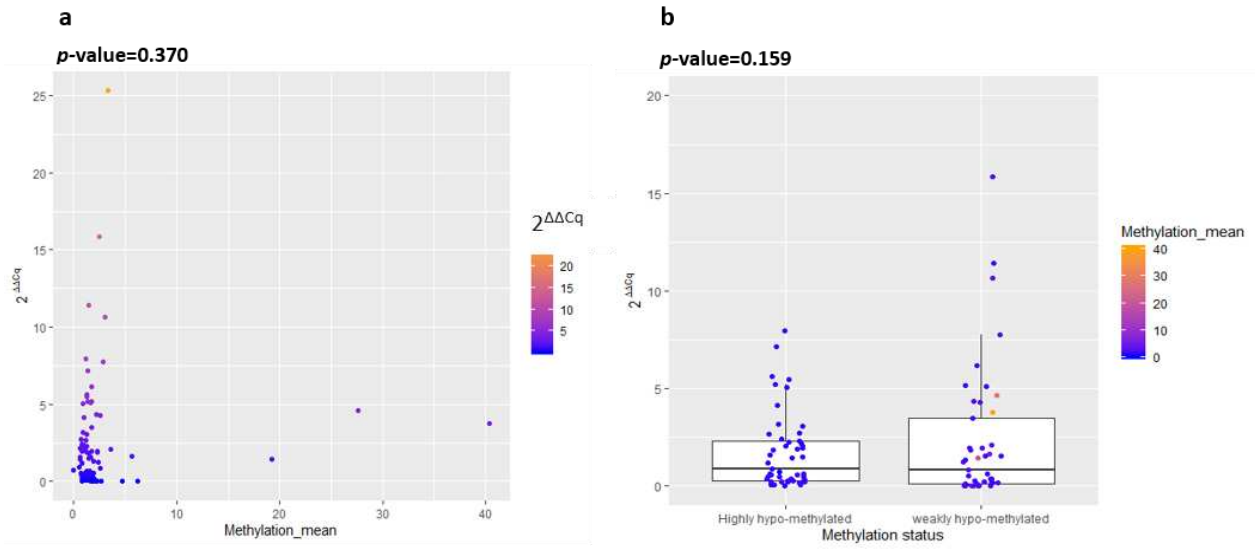

FIGURE 5